5th ECPMG Delft · 2024

Proceedings of the 5th ECPMG 2024
5th European Conference on Physical Modelling in Geotechnics
2-4 October 2024, Delft, the Netherlands

Understanding the soil mechanical response of tickler chain – seabed interaction for beam trawl fishing gears

B. Ghorai,
Indian Institute of Technology Madras, Chennai, India, bghorai@iitm.ac.in
Formerly with Delft University of Technology, Delft, The Netherlands, bithin.ghorai@gmail.com
N. J. Koorn, G. H. Keetels,
Delft University of Technology, Delft, The Netherlands, njkoorn@hotmail.com, G.H.Keetels@tudelft.nl

ABSTRACT: Advancement in tickler chain beam trawling requires precise estimation of seabed resistance to minimize marine habitat disturbance and fuel consumption of trawlers. Physical experiments to model seabed-structure interaction of fishing gear elements are prudent in designing less impactful and fuel-efficient gears. In this study, we developed a small-scale test setup, capable of towing multiple tickler chains in a flume filled with sandy soil and water to replicate beam-trawl gear elements in the sea. A series of model tests was performed to tow multiple chain elements on sandy sediments. Towing forces were evaluated for different parameters such as chain link diameter, tow velocity, angle of attack, penetration depth, soil particle size and relative density to investigate their influences on the mobilized soil resistance. Non-dimensional empirical relations were developed to estimate the soil mechanical drag resistance of prototype gears as a function of tow velocity and penetration depth. The method could be used to predict the vessel engine power and optimize performance of demersal fishing gears with improved catchability.

1 INTRODUCTION

The conventional method of beam trawl fishing with tickler chains has become increasingly important in the North Sea due to the European ban in electrical pulse fishing (Kraan et al., 2020). The method involves rigging a series of chains to catch flatfish species (*Solea solea*) living on the upper sediment layers of the seabed. As the energy requirement of the trawler depends on the hydrodynamical and geotechnical loads on the fishing net and supporting gear elements, understanding the physics involved in those interactions is necessary. Research in hydrodynamic response characteristics of trawl net and supporting gear elements are plenty in the literature (Prat et al., 2008; Bi et al., 2014; O'Neill and Ivanovic, 2016; Tang et al., 2017, 2018; Depestele et al., 2019; Rijnsdorp et al., 2020); however, limited attention is paid to the geotechnical interaction of fishing gears. Enerhaug (2011, 2012) demonstrated that towing speed and angle of attack of different ground gears (e.g., chains, rock-hoppers, bobbins and ropes) have considerable impacts on the towing resistance. It is also well envisaged from offshore pipeline ploughs (Cathie and Wintgens, 2001, Lauder et al., 2012, 2013) that the towing force on a blade for soil cutting is remarkably influenced by the sediment properties (e.g. mean particle size, permeability and relative density). The dynamics of beam trawl gear-seabed interaction with multiple tickler chains is like cutting the seafloor with a vertical blade (Miedema, 2017) and has not yet been investigated. This motivates to study the response of multiple chains towed across a soil layer, aiding optimized designs for reduced physical impact.

The beam trawling technique requires a cone-shaped net to be dragged on the seafloor at ~ 4.5 - 7 knots speed (equivalent to ~ 2.3 – 3.6 m/s) with several gear components including a steel beam (4.5 - 12 m length), a series of tickler chains and a ground rope. To minimize benthic disturbances on the seabed, estimation of gear penetration depth is essential (Lindeboom and De Groot, 1998, Depestele et al., 2016, 2019, Hiddink et al., 2017, De Borger et al., 2021 to name a few). Furthermore, predicting the vessel engine power to optimize the fuel efficiency is crucial for safe operation (Rijnsdorp et al., 2000). In this study, small-scale physical experiments were conducted to estimate the towing resistance of multiple chains dragged along a saturated sand bed. The steady-state forces were computed for a range of chain-soil parameters. Finally, a simple scaling relation was derived between the non-dimensional drag force and velocity from model test results to predict the towing resistance of beam trawl gear components.

2 MATERIALS AND METHODS

2.1 Experimental setup and procedure

Small-scale model tests were carried out with sections of tickler chain element in a water flume filled with sand. A test setup was built to tow multiple chain elements over a saturated bed of sandy soil at constant speed and penetration. Two types of model tickler chain element: light and heavy chain pattern were used. The factors that were considered during scaling of models (Enerhaug et al., 2012) are – chain length (l) and chain link diameter (d). A length factor, $\lambda_l = 60$ was used to reduce potential boundary effects (flume tank width $b = 40$ cm), and a diameter factor, $\lambda_d = 2$ was chosen to minimize particle size effects (d is significantly greater than the mean particle diameter d_{50}, Albiker et al., 2017).

Table 1. Parameter matrix for model tests.

Parameter	**Values***
Chain link diameter (d)	6 mm (light), 16 mm (heavy)
Mass of a single chain element (m)	0.48 kg, 1.8 kg
Tow velocity (v)	0.1 m/s, 0.3 m/s, 0.6 m/s
Angle of attack (α)	30°, 60°, 90°
Penetration depth (z)	12, 22, 32 mm [Light chain] 27, 37, 47 mm [Heavy chain]
Soil particle size (d_{50})	0.17 mm (Fine-grained), 0.26 mm (Coarse-grained)
Specific gravity (G)	2.65
Saturated density (ρ_s)	1700 kg /m^3 (Loose sand), 1961 kg /m^3 (Dense sand)

**Underlined values denote the reference case.*

The flume tank was partially packed with dry fine silica sand with mean grain size $d_{50} = 0.17$ mm to maintain a constant bed height of ~ 15 cm and partially filled with water (~ 10 cm over sand bed height) over a length of ~ 3.4 m to realize fully saturated soil condition. A mobile carriage with three pre-tensioned chain elements is mounted on top of the flume. The chains were dragged longitudinally at a constant speed along the flume length, whereas the vertical and lateral movements in soil were restrained. The test setup is explained in Figure 1 in a schematic manner. Three pairs of water-resistant force sensors with a maximum capacity of ~ 1kN (combined error 0.02%) were used to measure the steady-state towing force normal to the chain axis. The output signals were recorded and stored in a Data Acquisition System (DAS) for analysis (Figure 1). The experiments were conducted in the water flume facility available at TU Delft, Netherlands (Figure 2). For each parameter listed in Table 1, multiple test runs were performed to ensure repeatability of results.

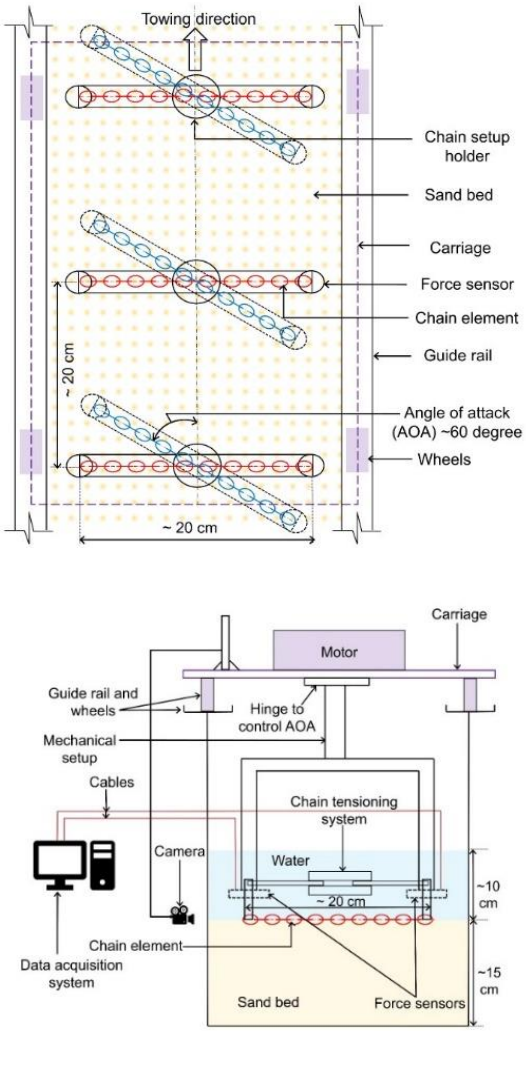

Figure 1. Schematic diagram of experimental setup (a) top view and (b) front view.

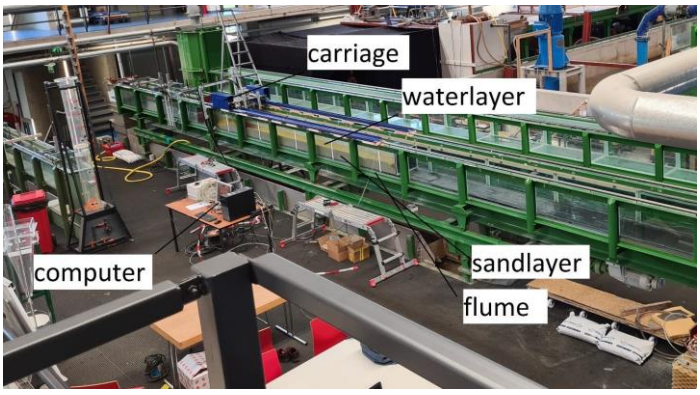

Figure 2. Water flume facility at TU Delft adapted for beam trawl gear experiment.

3 RESULTS AND DISCUSSIONS

A reference case was initially defined to study the influence of individual chain-soil parameter (e.g. velocity, angle of attack, chain link diameter, penetration depth, soil particle size and relative density). Results for a typical case are presented in the subsequent sections.

3.1 Towing speed

Figure 3 shows the steady-state towing force responses in saturated fine sand for three velocities v = 0.1, 0.3 and 0.6 m/s. As can be seen, the force increases with the velocity for a given chain and soil property, however, similar responses were recorded at higher speeds. Tow velocities of v > 0.6 m/s could not be tested as it resulted in wave generation and associated turbulence during towing in the flume tank.

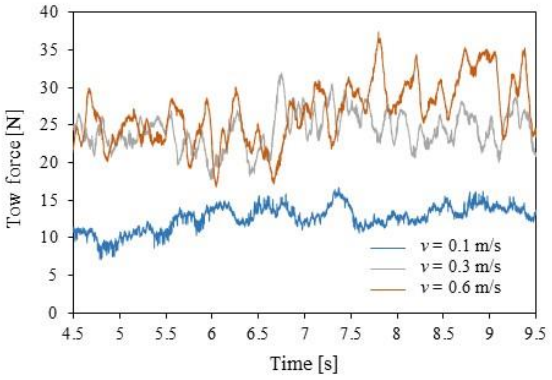

Figure 3. Steady-state force for different tow velocities.

3.2 Chain link diameter

Figure 4 illustrates the average tow force required to drag the chains in saturated fine sand for two different link sizes.

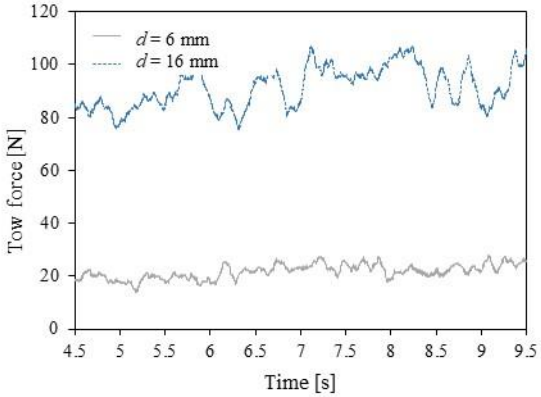

Figure 4. Steady-state force for different chain link sizes.

The force increases with the chain link size owing to the greater submerged weight. As the chain size increases, more volume of soil is pushed forward during towing (bulldozing effect), and greater passive resistance is mobilized.

3.3 Angle of attack

Three different angles of attack, α = 90°, 60° and 30° were considered to account for the catenary shape effect of tickler chains in beam trawling. The definitions of α and tow force components are depicted in Figure 5. The average steady-state force is given by:

$$F_t = F_n \left[\sin\alpha + \tan\varphi' \cos\alpha \right] \quad (1)$$

Where, F_t is the total towing force, F_n is the normal component and $F_n \tan\phi'$ is the tangential component (ϕ' being the soil effective friction angle). Figure 6 presents the steady-state tow force variations for different angles. It was observed that less soil resistance is mobilized when the chains are dragged at low angles.

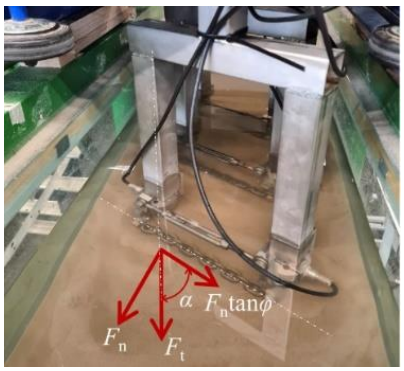

Figure 5. Force components for an angle of attack.

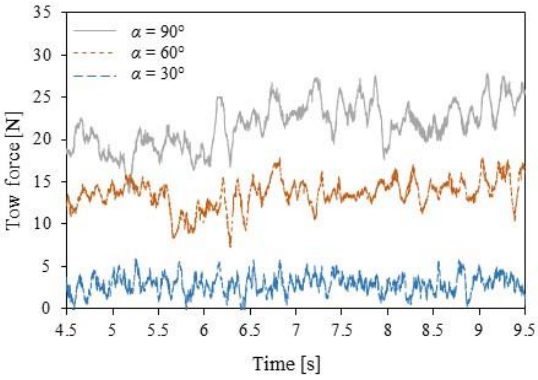

Figure 6. Steady-state force at various angles of attack.

3.4 Penetration depth

The initial penetration depth (z_i) is defined as the embedded vertical length of a chain link into the soil (Figure 7). Note that the initial penetration depth is a function of the chain link diameter and varies considerably for various link sizes (Table 1). To evaluate the effect of chain penetration depth, circular

metal discs (D1, D2, and D3, each having 10 mm thickness) were inserted between the carriage and the chain holder (Figure 7). The reference case (one disc) is marked with $z_i = 0$ that corresponds to a penetration depth of 12 mm for 6 mm diameter chain (light). With each additional disk, the penetration increased by 10 mm, i.e. $z_i = 10$ (for 22 mm penetration) and $z_i = 20$ (for 32 mm penetration).

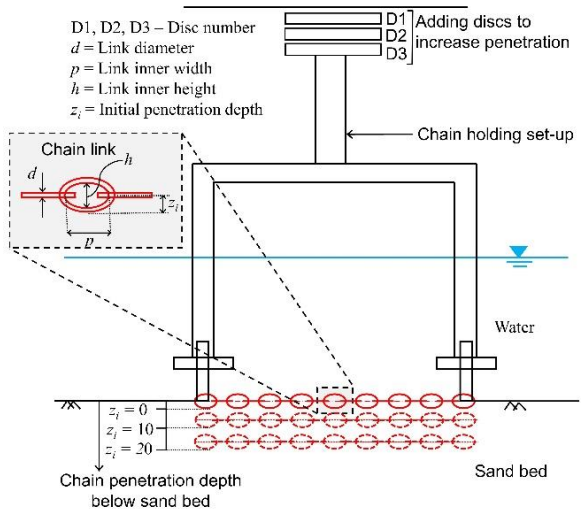

Figure 7. Schematic of chain penetration depth with disc arrangement.

The steady-state forces are compared in Figure 8. It was observed that the average tow force increases with penetration depth for a given chain diameter and velocity. This is because higher the penetration, larger the volume of soil moving in front of the chains and greater the force required for towing.

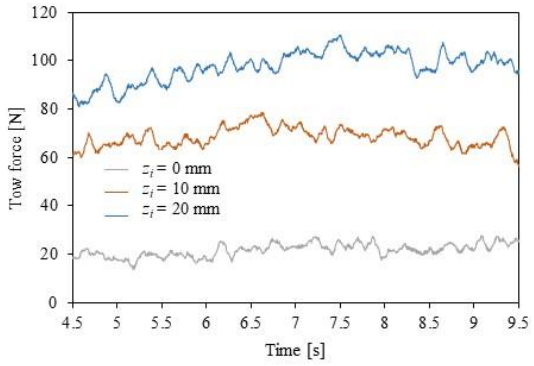

Figure 8. Steady-state force for different penetration depths.

3.5 Soil parameters

The effects of soil particle size and relative density were investigated. Two different grain sizes of industrially processed silica sand (supplied by Sibelco from Belgium) were considered – (i) fine-grained sand (Mol 34) and (ii) coarse-grained sand (Mol 32). The mean particle diameter of Mol 34 and Mol 32 type sand was $d_{50} = 0.17$ mm and 0.26 mm, respectively. As d/d_{50} ratios were in the range of ~ 35 - 94 for fine-grained soil and ~ 23 to 62 for coarse-grained soil, scale effects are expected to be minimal. Two extreme packing configurations with relative density R_D ~ 0-10% (loose bed, bed height = 15 cm) and 85% (dense bed, bed height = 13 cm) were considered. Results for various cases are compared in Figure 10 (Ghorai et al., 2024).

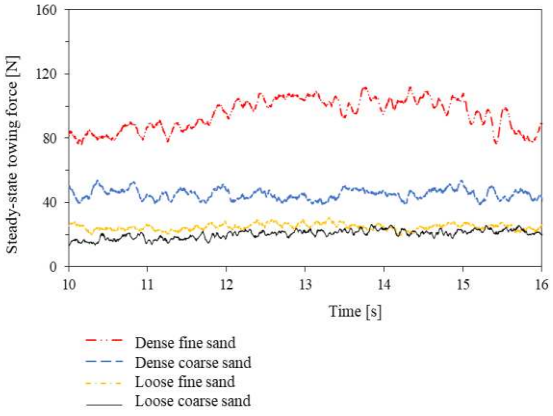

Figure 10. Steady-state tow force in sandy soil with different grain sizes and relative densities.

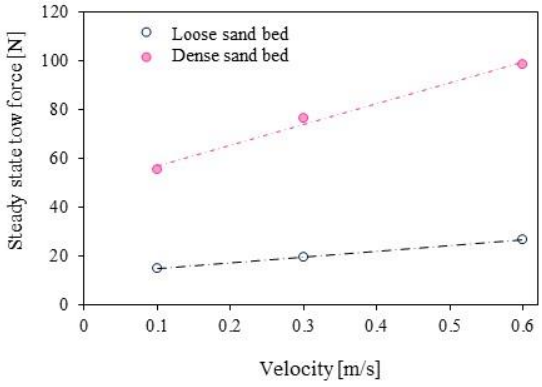

Figure 11. Steady-state tow force for different soil packing configurations in fine-grained soil.

It was observed that the steady-state force required to tow the chains is almost similar for two different grains in loose condition. However, in dense soil, the average force was increased by nearly 2.7 times when dragged over fine-grained particles. This is due to the fact that effective friction angle increases with soil relative density at low confining stress under drained shearing (Bolton, 1986; Chakraborty and Salgado, 2010), and therefore, the passive soil pressure increases leading to increased towing resistance (Cathie and Wintgens, 2001, Depestle et al., 2016).

The mean soil resistances were also calculated at different towing speeds and compared in Figure 11 for

the fine-grained sand (Ghorai et al., 2024). The average force in dense fine sand seemed to increase by ~3.7 times compared to the loose fine sand due to change in the void ratio of soil by ~ 44%. On sandy fishing grounds the loose state is expected to be more representative as the top layer of sediments is regularly sheared by ocean waves and currents.

3.6 Scaling hypothesis

The towing force F_t is controlled by the saturated soil density (ρ_s), towing speed (v), penetration depth (z_i), and gravitational acceleration (g). According to the Buckingham Π theorem, two non-dimensional groups can be formed as the problem is governed by 5 independent variables and 3 fundamental units (mass, time and length). The first group represents the average towing force on the chain system normalized by the weight of a soil beam (Guo and Stolle, 2005) that needs to be lifted to make passage for the chains:

$$\bar{F}_t = \frac{F_t}{\rho_s g z_i^2 l} \qquad (2)$$

The second group denotes the normalized tow velocity in terms of Froude number F_r (with penetration depth as the characteristic length):

$$F_r = \frac{v}{\sqrt{g z_i}} \qquad (3)$$

The geotechnical drag resistance of chains in the limit of low velocity could be alternatively described using the earth pressure theory (Verruijt, 2006) considering passive soil pressure coefficient K_p. Equation (2) can be modified to:

$$\bar{F}_t = \frac{F_t}{K_p \rho_s g z_i^2 l} \qquad (4)$$

Figure 12 illustrates the non-dimensional force as a function of Froude number for various cases. The difference in steady-state towing forces is evident for the loose and dense soil state (Fig 12a). This could be attributed to higher friction angle mobilized at low confining stress in dense sand (Bolton, 1986), leading to greater passive resistance.

To understand the shielding effect on chain resistance, the force on the front chain is plotted with a multiplication factor of 3 (= number of chains). The total estimated force on the system appeared to be large due to contribution from the front chain only, where the soil was densely compacted. Following the passage of first chain, the soil particles were suspended into the water column and then deposited gradually onto the bed resulted in a loose packing [compare the dense fine sand case with the dense fine sand for 3 x front chain in Figure 12a]. We used two different passive soil pressure coefficients with respect to the loose bed condition ($K_p/K_{p,ref}$ = 2.9 and 5.2) for normalization. The coefficient K_p depends on effective the friction angle, ϕ' and thus different friction angles can be mobilized for different soil relative densities. Figure 12(b) demonstrates the non-dimensional tow force corrected for various K_p.

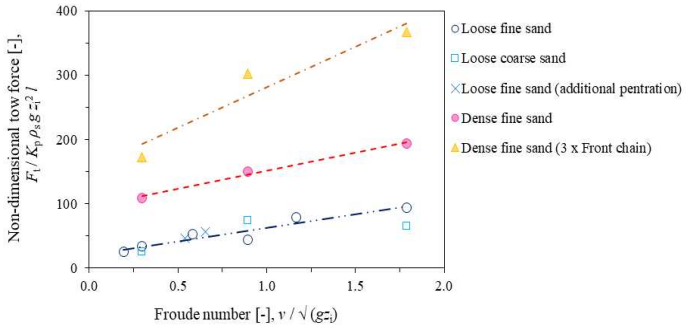

(a)

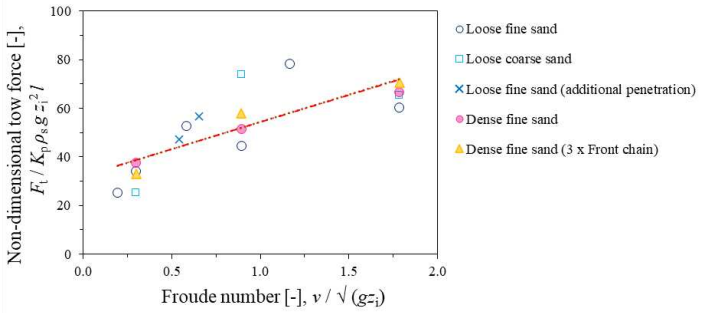

(b)

Figure 12. Normalized tow force as a function of Froude number: (a) for various soil conditions, (b) accounting for different passive earth pressure coefficients.

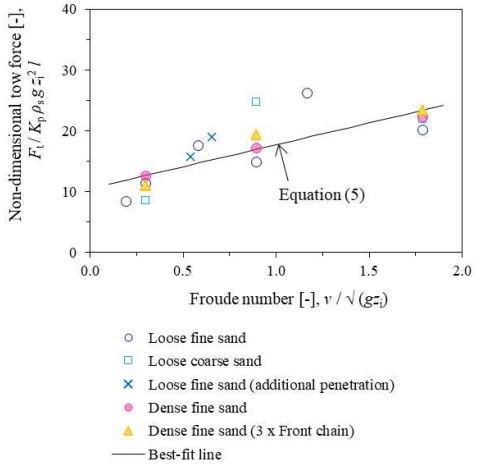

Figure 13. Non-dimensional tow force as a function of Froude number for various tickler chain - seabed configuration.

However, it is important to note that the non-dimensional forces are estimated with respect to $K_{p,ref}$ = 1.0. In our experiments, loose fine-grained sediment with $\phi' = 30^{\circ}$ implying K_p = 3 represents the reference case. Therefore, the normalized tow forces were accurately predicted using a scale factor 3 (Figure 13). A best-fit curve of the linear form was used to translate these results from model scale to prototype scale:

$$\bar{F}_t = a + bF_r \qquad (5)$$

Where, a = 10.5 and b = 7.2 are coefficients obtained from linear regression analysis (R^2 ~ 0.7).

4 CONCLUSIONS

The physical interaction of beam trawl gear components with sandy sediment was studied by means of small-scale model experiments. A system of multiple tickler chains was dragged in a water-soil flume to understand the impact of various parameters (tow velocity, chain diameter, angle of attack, penetration depth, soil grain size, relative density) on the steady-state towing resistance. Results were presented in non-dimensional charts to enable calculation for prototype gear elements. It should be noted that the penetration depth evolves during dragging of the beam trawl gear components in the sea unlike our experiments where the penetration depth is fixed during towing. An empirical relation was proposed to predict the non-dimensional tow force as a function of towing speed and penetration depth. The framework could be applied to other type of sea beds such as soft clay and gravel for future studies to assess the towing resistance of demersal fishing gears.

ACKNOWLEDGEMENTS

The authors are grateful for the financial support provided by the NWO (Dutch Research Council) project - Numerical modelling of demersal fishing net systems for design optimization (FishNetSim) in The Netherlands [project number 18529]. Our sincere thanks to the Faculty of Civil Engineering and Geosciences at TU Delft for allowing us to conduct experiments in the Hydraulic Engineering Laboratory. A special thanks to Pieke Molenaar and Justin Tiano of Wageningen Marine Research for their support in providing details of beam trawl gear components and development of models. Thanks, are also extended to André van den Bosch and Ed Stok for their practical assistance in the experiments at TU Delft.

REFERENCES

Albiker, J., Achmus, M., Frick, D., and Flindt, F. (2017). 1 g model tests on the displacement accumulation of large-diameter piles under cyclic lateral loading. *Geotechnical Testing Journal*, 40(2): 173–184. https://doi.org/10.1520/GTJ20160102

Bi, C. W., Zhao, Y. P., Dong, G. H., Xu, T. J., and Gui, F. K. (2014). Numerical simulation of the interaction between flow and flexible nets. *Journal of Fluids and Structures,* 45: 180-201. https://doi.org/10.1016/j.jfluidstructs.2013.11.015

Bolton, M. D. (1986). The strength and dilatancy of sands. *Géotechnique*, 36(1): 65–78. https://doi.org/10.1680/geot.1986.36.1.65

Cathie, D. N., and Wintgens, J. F. (2001). Pipeline trenching using plows: performance and geotechnical hazards. *Proceedings of the Offshore Technology Conference* (OTC), OnePetro. https://doi.org/10.4043/13145-MS

Chakraborty, T., and Salgado, R. (2010). Dilatancy and shear strength of sand at low confining pressures. *Journal of Geotechnical and Geoenvironmental Engineering*, 136(3): 527-532. https://doi.org/10.1061/(ASCE)GT.1943-5606.0000237

De Borger, E., Tiano, J., Braeckman, U., Rijnsdorp, A. D., and Soetaert, K. (2021). Impact of bottom trawling on sediment biogeochemistry: a modelling approach. *Biogeosciences*, 18(8): 2539–2557. https://doi.org/10.5194/bg-18-2539-2021

Depestele, J., Degrendele, K., Esmaeili, M., Ivanović, A., Kröger, S., O'Neill, F. G., Parker, R., Polet, H., Roche, M., Teal, L. R., Vanelslander, B., and Rijnsdorp, A. D. (2019). Comparison of mechanical disturbance in soft sediments due to tickler-chain Sum Wing trawl versus electro-fitted Pulse Wing trawl. *ICES Journal of Marine Science*, 76(1): 312–329. https://doi.org/10.1093/icesjms/fsy124.

Depestele, J., Ivanović, A., Degrendele, K., Esmaeili, M., Polet, H., Roche, M., Summerbell, K., Teal, L. R., Vanelslander, B., and O'Neill, F. G. (2016). Measuring and assessing the physical impact of beam trawling. *ICES Journal of Marine Science,* 73: 15–26. https://doi.org/10.1093/icesjms/fsv056

Enerhaug, B. (2011). Contact forces between seabed and fishing gear components. *Proceedings of the 10th International Workshop on Methods for the Development and Evaluation of Maritime Technologies* (DEMAT' 11), M. Paschen (ed.), Shaker Verlag Aachen, Vol. 7, pp. 237-246.

Enerhaug, B., Ivanović, A., O'Neill, F., and Summerbell, K. (2012). Friction forces between seabed and fishing gear components. *Proceedings of the ASME 2012 31st International Conference on Ocean, Offshore and Arctic Engineering*, ASME, Vol. 7, pp. 61-68. https://doi.org/10.1115/OMAE2012-83395

Ghorai, B., Tiano, J., Molenaar, P., Soetaert, K., and Keetels, G. (2024). Predicting the penetration depth and towing resistance of beam trawl fishing gears in sand. *Marine Georesources & Geotechnology*, (*In press*) https://doi.org/10.1080/1064119X.2024.2361009

Guo, P. J., and Stolle, D. F. E. (2005). Lateral pipe-soil interaction in sand with reference to scale effect. *Journal of Geotechnical and Geoenvironmental Engineering*, 131(3): 338-349. https://doi.org/10.1061/(ASCE)1090-0241(2005)131:3(338)

Hiddink, J. G., Jennings, S., Sciberras, M., Szostek, C. L., Hughes, K. M., Ellis, N., Rijnsdorp, A. D., McConnaughey, R. A., Mazor, T., Hilborng, H., Collie, J. S., Pitcher, C. R., Amoroso, R. O., Parma, A. M., Suuronen, P., and Kaiser, M. J. (2017). Global analysis of depletion and recovery of seabed biota after bottom trawling disturbance. *Proceedings of the National Academy of Sciences,* 114(31): 8301–8306. https://doi.org/10.1073/pnas.1618858114

Kraan, M., Groeneveld, R., Pauwelussen, A., Haasnoot, T., and Bush, S. R. (2020). Science, subsidies and the politics of the pulse trawl ban in the European Union. *Marine Policy*, Vol. 118, pp: 103975. https://doi.org/10.1016/j.marpol.2020.103975

Lauder, K. D., Brown, M. J., Bransby, M. F., and Boyes, S. (2013). The influence of incorporating a forecutter on the performance of offshore pipeline ploughs. *Applied Ocean Reseaerch*, 39: 121-130. http://dx.doi.org/10.1016/j.apor.2012.11.001

Lauder, K. D., Brown, M. J., Bransby, M. F., and Gooding, S. (2012). Variation of tow force with velocity during offshore ploughing in granular materials. *Canadian Geotechnical Journal*, 49(11): 1244-1255. https://doi.org/10.1139/t2012-086

Lindeboom, H. J., and De Groot, S. J. (1998). The effects of different types of fisheries on the North Sea and Irish Sea benthic ecosystems (IMPACT-II). - Report 1998-1/RIVO-DLO Report C003/98. Netherlands Institute for Sea Research, Texel, The Netherlands, 404.

Miedema, S. A. (2017). *The Delft sand, clay & rock cutting model 3rd edition*. IOS Press BV, Amsterdam, The Netherlands.

O'Neill, F. G., and Ivanović, A. (2016). The physical impact of towed demersal fishing gears on soft sediments. *ICES Journal of Marine Science*, 73: 5-14. https://doi.org/10.1093/icesjms/fsv125

Prat, J., Antonijuan, J., Folch, A., Sala, A., Lucchetti, A., Sardà, F., and Manuel, A. (2008). A simplified model of the interaction of the trawl warps, the otterboards and netting drag. *Fisheries Research*, 94(1): 109-117. https://doi.org/10.1016/j.fishres.2008.07.007

Rijnsdorp, A. D., Dol, W., Hoyer, M., and Pastoors, M. A. (2000). Effects of fishing power and competitive interactions among vessels on the effort allocation on the trip level of the Dutch beam trawl fleet. *ICES Journal of Marine Science*, 57(4): 927–937. https://doi.org/10.1006/jmsc.2000.0580

Rijnsdorp, A. D., Hiddink, J. G., van Denderen, P. D., Hintzen, N. T., Eigaard, O. R., Valanko, S., Bastardie, F., Bolam, S. G., Boulcott, P., Egekvist, J., Garcia, C., van Hoey, G., Jonsson, P., Laffargue, P., Nielsen, J. R., Piet, G. J., Sköld, M., and van Kooten, T. (2020). Different bottom trawl fisheries have a differential impact on the status of the North Sea seafloor habitats. *ICES Journal of Marine Science*, 77(5): 1772–1786. https://doi.org/10.1093/icesjms/fsaa050

Tang, M. F., Dong, G. H., Xu, T. J., Zhao, Y. P., and Bi, C. W. (2017). Numerical simulation of the drag force on the trawl net. *Turkish Journal of Fisheries and Aquatic Sciences,* 17: 1219-1230. https://www.trjfas.org/uploads/pdf_1114.pdf

Tang, M. F., Dong, G. H., Xu, T. J., Zhao, Y. P., Bi, C. W., and Guo, W. J. (2018). Experimental analysis of the hydrodynamic coefficients of net panels in current. *Applied Ocean Research*, 79: 253-261, https://doi.org/10.1016/j.apor.2018.08.009

Verruijt, A. (2006). *Offshore soil mechanics*. Delft University of Technology, The Netherlands. OffshoreSMBook.pdf (verruijt.net)